



Angiotensin Converting Enzyme-2 Therapy Improves Liver Fibrosis and Glycemic Control in Diabetic Mice With Fatty Liver

Indu G. Rajapaksha ,¹ Lakmie S. Gunarathne ,¹ Khashayar Asadi,² Ross Laybutt,^{3,4} Sof Andrikopoulos,¹ Ian E. Alexander,⁵ Mathew J. Watt,⁶ Peter W. Angus,^{1,7} and Chandana B. Herath^{1,8,9}

Nonalcoholic fatty liver disease (NAFLD) is the most common cause of chronic liver disease and is frequently associated with type 2 diabetes. However, there is no specific medical therapy to treat this condition. Angiotensin-converting enzyme 2 (ACE2) of the protective renin angiotensin system generates the antifibrotic peptide angiotensin-(1-7) from profibrotic angiotensin II peptide. In this study, we investigated the therapeutic potential of ACE2 in diabetic NAFLD mice fed a high-fat (20%), high-cholesterol (2%) diet for 40 weeks. Mice were given a single intraperitoneal injection of ACE2 using an adeno-associated viral vector at 30 weeks of high-fat, high-cholesterol diet (15 weeks after induction of diabetes) and sacrificed 10 weeks later. ACE2 significantly reduced liver injury and fibrosis in diabetic NAFLD mice compared with the control vector injected mice. This was accompanied by reductions in proinflammatory cytokine expressions, hepatic stellate cell activation, and collagen 1 expression. Moreover, ACE2 therapy significantly increased islet numbers, leading to an increased insulin protein content in β -cells and plasma insulin levels with subsequent reduction in plasma glucose levels compared with controls. *Conclusion:* We conclude that ACE2 gene therapy reduces liver fibrosis and hyperglycemia in diabetic NAFLD mice and has potential as a therapy for patients with NAFLD with diabetes. (*Hepatology Communications* 2022;6:1056-1072).

Nonalcoholic fatty liver disease (NAFLD) is the most common chronic liver disease worldwide.⁽¹⁻³⁾ A subset of patients with NAFLD will develop its severe inflammatory form, nonalcoholic steatohepatitis (NASH), with histological changes of lobular inflammation and hepatocellular ballooning.^(4,5) It has been estimated that

approximately 20% of patients with NASH will progress to liver cirrhosis and/or hepatocellular carcinoma,^(6,7) and NAFLD/NASH-associated cirrhosis is now the most common indication for liver transplantation in the United States.⁽⁸⁾ Thus, there is a major need to develop effective treatments for this condition.

Abbreviations: AAV, adeno-associated virus; ACE, angiotensin converting enzyme; ACE2, angiotensin converting enzyme 2; ALB, human albumin; ALP, alkaline phosphatase; ALT, alanine aminotransferase; Ang, angiotensin; ANOVA, one-way analysis of variance; ApoE, apolipoprotein E; AST, aspartate transaminase; AT1-R, angiotensin II type 1 receptor; BSA, bovine serum albumin; COL1A1, collagen 1 α 1; CTGF, connective tissue growth factor; DAB, 3,3-diaminobenzidine; DM, diabetes mellitus; ECM, extracellular matrix protein; hAAT, human alpha-1 antitrypsin; HFHC, high-fat, high-cholesterol; HSC, hepatic stellate cell; IL-6, interleukin-6; MasR, Mas receptor; mRNA, messenger RNA; NAFLD, nonalcoholic fatty liver disease; NASH, nonalcoholic steatohepatitis; rAAV/8-ACE2-, adeno-associated viral vector carrying mouse ACE2; RAS, renin angiotensin system; RT, room temperature; STZ, streptozotocin; TGF- β 1, transforming growth factor β 1; α -SMA, alpha-smooth muscle actin.

Received August 18, 2021; accepted December 4, 2021.

Supported by the Australian National Health and Medical Research Council (APP1062372 and APP1124125).

© 2021 The Authors. *Hepatology Communications* published by Wiley Periodicals LLC on behalf of American Association for the Study of Liver Diseases. This is an open access article under the terms of the Creative Commons Attribution-NonCommercial-NoDeriv License, which permits use and distribution in any medium, provided the original work is properly cited, the use is non-commercial and no modifications or adaptations are made.

View this article online at wileyonlinelibrary.com.

DOI 10.1002/hep4.1884

Potential conflict of interest: Nothing to report.

The renin angiotensin system (RAS) is activated as part of the wound-healing response to chronic liver injury and plays a central role in the pathogenesis of hepatic fibrosis.⁽⁹⁻¹¹⁾ The “classical” axis of the RAS includes angiotensin-converting enzyme (ACE), which converts the biologically inactive decapeptide angiotensin I (Ang I) to the octapeptide angiotensin II (Ang II), the primary effector peptide of this axis, and the Ang II type I receptor (AT1-R). Ang II causes vasoconstriction, inflammation, wound healing, and fibrogenesis through the AT1-R. However, with the discovery of the ACE homologue, ACE2, understanding of the RAS has changed.⁽¹²⁾ ACE2 breaks down Ang II to the peptide, angiotensin-(1-7) (Ang-[1-7]),^(10,13) which acts through its receptor Mas (MasR). This ACE2/Ang-(1-7)/MasR axis is known as the alternate or protective axis of the RAS.^(10,14) ACE2 and its effector heptapeptide Ang-(1-7) are activated in both experimental and human chronic liver disease and counter-regulate fibrogenesis and other deleterious effects of Ang II.^(10,13,15) Thus, this protective axis of the RAS serves as a potential target for therapeutic intervention in chronic liver diseases.⁽¹⁶⁾

Our recent studies showed that overexpression of ACE2 in the liver ameliorates biliary fibrosis in the long-term multiple drug resistance protein-2 knock-out mouse model that develops lesions resembling those of human primary sclerosing cholangitis.⁽¹⁰⁾ Additionally, we have characterized the therapeutic effects of ACE2 in short-term animal models with early NAFLD.⁽¹³⁾ In the current study, we sought to expand these observations and determine the therapeutic effect of ACE2 overexpression in a long-term animal model with severe NAFLD/NASH. Because

the presence of diabetes increases liver fibrosis in NAFLD,^(17,18) we also examined the effects of ACE2 overexpression in a chronic dietary model of NAFLD exacerbated by diabetes.⁽¹⁹⁾

Materials and Methods

ANIMALS AND EXPERIMENTAL DESIGN

All animals were housed with a 12-hour light-dark cycle at room temperature (22°C-24°C) with water and standard mouse chow *ad libitum*. Experimental procedures were approved by the Animal Ethics Committee of Austin Health and performed according to the National Health and Medical Research Council of Australia Guidelines for animal experimentation.

The experimental design is shown in Figure 1A. Six-week-old to 8-week-old C57BL/6 mice were randomly assigned into four groups. They were fed a high-fat, high-cholesterol (HFHC) diet (21% fat and 2% cholesterol)⁽²⁾ for 40 weeks. Hyperglycemia exacerbates liver fibrosis/cirrhosis in animal models and humans with NAFLD.⁽²⁰⁾ To develop a mouse model with advanced NASH, three groups of HFHC fed animals were rendered diabetic (diabetes mellitus [DM]) using two consecutive daily injections of streptozotocin (STZ; 65 mg/kg) (Sigma-Aldrich, St. Louis, MO)^(19,21) at 15 weeks of HFHC diet. One group was injected intraperitoneally with a liver-specific adeno-associated vector expressing mouse ACE2 (rAAV2/8-ACE2) (n = 10), and the second group received the control vector rAAV2/8-ALB

ARTICLE INFORMATION:

From the ¹Department of Medicine, The University of Melbourne, Austin Health, Heidelberg, VIC, Australia; ²Anatomical Pathology, Austin Health, Heidelberg, VIC, Australia; ³Garvan Institute of Medical Research, Sydney, NSW, Australia; ⁴St. Vincent's Clinical School, University of New South Wales, Sydney, NSW, Australia; ⁵School of Medicine, University of Sydney, Children's Medical Research Institute, Sydney, NSW, Australia; ⁶Department Anatomy and Physiology, The University of Melbourne, Melbourne, VIC, Australia; ⁷Department Gastroenterology, Austin Health, Heidelberg, VIC, Australia; ⁸South Western Sydney Clinical School, Faculty of Medicine, University of New South Wales, Sydney, NSW, Australia; ⁹Ingham Institute for Applied Medical Research, Liverpool, NSW, Australia.

ADDRESS CORRESPONDENCE AND REPRINT REQUESTS TO:

Chandana B. Herath, Ph.D.
Ingham Institute for Applied Medical Research
1, Campbell St

Liverpool, NSW 2170, Australia
E-mail: c.herath@unsw.edu.au
Tel.: +61-2-8738-9057

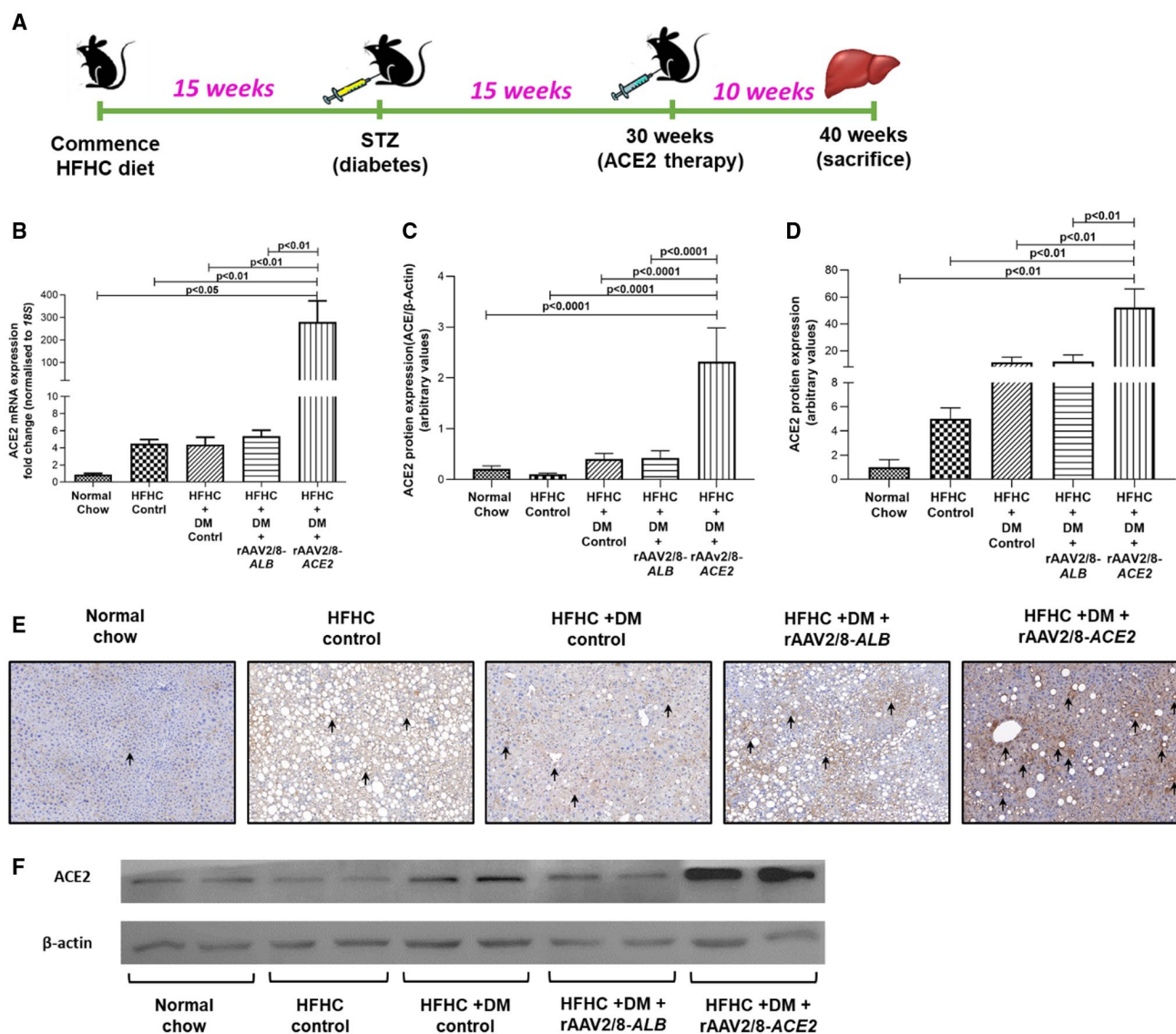


FIG. 1. Hepatic ACE2 mRNA and protein expression at an advanced stage of NAFLD. (A) Schematic representation of study design. ACE2 mRNA expression (B) and protein content as shown by immunohistochemical (C,E) and western blotting (D,F) were significantly up-regulated in the liver of ACE2-treated mice compared with all other groups. ACE2 is predominantly localized to hepatocytes (E; arrows). The mRNA expression data have been normalized to endogenous control gene, 18S, and healthy control group was given an arbitrary value of 1. Each bar represents the mean \pm SEM profile of 5 (normal chow) or 10 (HFHC groups) and 10-15 (HFHC-fed diabetic groups) mice per treatment group as calculated by one-way ANOVA with Tukey's multiple comparison test. (E) Immunohistochemical images (20 \times in Fiji Image J) with arrows pointing to stained hepatocytes.

expressing human albumin (n = 10) at 30 weeks of HFHC diet. Each animal received a single dose of freshly prepared 1×10^{11} vector genomes (vg) of the viral vector. Animals in both groups were sacrificed after 40 weeks of HFHC diet (10 weeks following vector injection) (Fig. 1A). The third group was sacrificed after 40 weeks of HFHC diet without vector intervention to serve as a diabetic disease

control (n = 10). The fourth group (n = 10), which was sacrificed after 40 weeks, served as the nondiabetic HFHC diet control group. Additionally, a fifth group of age-matched C57BL/6 mice fed a normal chow diet served as healthy controls (n = 5). To make comparisons of plasma insulin and glucose levels before and after ACE2 therapy, three additional groups of mice (i.e., normal chow, HFHC fed

nondiabetic, and HFHC fed diabetic) were killed at 30 weeks of the diets. All animals were euthanized under lethal anesthesia induced by pentobarbitone (120 mg/kg) for blood and tissue collection.

VIRAL VECTOR PREPARATION

We constructed a pseudo-serotyped vector with murine liver trophic adeno-associated virus (AAV) serotype 8 capsid and liver-specific alipoprotein E (ApoE)/human alpha-1 antitrypsin (hAAT) enhancer-promoter driving mouse ACE2 expression (rAAV2/8-ACE2) and control AAV vector carrying human serum albumin (rAAV2/8-ALB) (kindly provided by A/Prof. Alexandra Sharland, University of Sydney), as we have previously described.^(10,13,22)

BIOCHEMICAL ASSESSMENT OF LIVER FUNCTION AND HEPATIC TRIGLYCERIDE CONTENT

Refer to the Appendix 1 for details of the procedure.

FIBROSIS ASSESSMENT

Quantification of Hepatic Messenger RNA Expression

Liver RNA extraction, complementary DNA synthesis, and quantitative polymerase chain reaction (PCR) were carried out as previously described.⁽²³⁾

Histological Assessment of Liver Injury and Fibrosis

Four μm -thick paraffin-embedded liver tissue sections were mounted on silane-coated glass slides and stained with hematoxylin and eosin (H&E) and picrosirius red (BioScientific, Sydney, Australia) as described previously.⁽²³⁾ Hematoxylin and eosin, and picrosirius red-stained sections were assessed by a pathologist blinded to the treatments and scored using the “Metavir” scoring system. In addition, H&E-stained sections were quantified for both macrosteatosis and microsteatosis by the pathologist.

Liver fibrosis was assessed using picrosirius red-stained liver sections with 10 selected fields per section quantified for collagen at $\times 200$ magnification, as

described by us previously.⁽²³⁾ The picrosirius staining was also used to determine the “stage of fibrosis” considering the severity of fibrosis⁽²⁴⁾ with stage 1 (zone 3 pericellular fibrosis [focal or extensive]), stage 2 (zone 3 pericellular fibrosis [focal or extensive] and portal fibrosis (focal or extensive), stage 3 (bridging fibrosis [focal or extensive]), and stage 4 (cirrhosis, \pm foci of residual pericellular fibrosis).

ACE2 AND α -SMOOTH MUSCLE ACTIN IMMUNOHISTOCHEMISTRY

ACE2

Staining was also performed on 4- μm sections of paraffin-embedded mouse liver/pancreas tissue mounted on silane-coated glass slides. Heat-induced antigen retrieval was performed using citrate buffer in a microwave. Endogenous peroxidase activity in the liver specimens was removed by application of peroxidase block solution at room temperature (RT) for 5 minutes. The primary antibody to ACE2 (Abcam) at a concentration of 1:1,500 Tris-HCl containing 1% bovine serum albumin (BSA; Trace Biosciences, New Zealand) was applied, and the slides and were incubated overnight at 4°C.

Alpha-Smooth Muscle Actin

The biotinylated primary antibody to alpha-smooth muscle actin (α -SMA; Monoclonal 1A4) (Dako, Agilent Technologies, Santa Clara, CA) at a concentration of 1 in 50 in Tris-HCl containing 1% BSA (Trace Biosciences) was applied, and the slides and were left at RT for 15 minutes. Once the incubation with each primary antibody was completed, the sections were washed using Milli-Q water and 1 \times PBS, and incubated with streptavidin peroxidase at RT for 15 minutes. Sections were again washed with Milli-Q water and 1 \times PBS, and peroxidase conjugates were subsequently localized using 3,3-diaminobenzidine (DAB) + substrate chromogen (Sigma-Aldrich) at RT for 15 minutes. The relative staining in each group was determined by computerized quantification (Fiji Image J) in a total of 10 fields per liver/pancreas sample at $\times 200$ magnification and averaged in a blinded fashion.

Refer to the Appendix 1 for details of each procedure.

ASSESSMENT OF FASTING PLASMA GLUCOSE AND INSULIN

Mice were fasted for 6 hours, anesthetized, and blood was collected by heart puncture. Plasma glucose and insulin levels were measured using GM7 Analox glucose analyzer (Helena Laboratories, Beaumont, TX) and Alpco mouse insulin ultrasensitive enzyme-linked immunosorbent assay (r-biopharm, Australia), respectively.

INSULIN IMMUNOHISTOCHEMISTRY AND QUANTIFICATION OF INSULIN CONTENT IN PANCREATIC TISSUE SECTIONS

Pancreatic tissue was collected in 4% paraformaldehyde solution for 24 hours and transferred to 10% sucrose in 1 × PBS until used for paraffin embedding. One to 2 days before paraffin embedding, the tissues were transferred to 70% alcohol. The staining was performed on 4- μ m sections of paraffin-embedded mouse pancreatic tissue mounted on silane-coated glass slides. Specimens were dewaxed thrice in 100% histolene for 3 minutes each and dehydrated in graded ethanol (100%, 90%, and 70% ethanol for 2 minutes each). The sections were then washed in distilled water. The peroxidase block was performed by application of 3% hydrogen peroxide at RT for 5 minutes. The sections were washed with distilled water and then with 1 × PBS. The tissue sections were incubated with serum-free protein block (Dako) for 5 minutes at RT. The excess protein block was tipped off and blotted around the tissue section. The biotinylated primary antibody to insulin (polyclonal guinea pig anti-insulin) (Dako) at a concentration of 1 in 100 in antibody diluent (Dako) was applied and the slides were incubated in incubation chambers overnight at 4°C. They were washed in two changes of 1 × PBS, 5 minutes each, then incubated with streptavidin conjugated with peroxidase (DAB; Dako) at RT for 15 minutes. The sections were washed two times with 1 × PBS, 5 minutes each, and stained with hematoxylin (Sigma-Aldrich) as described elsewhere.⁽¹⁵⁾ Insulin staining in each group was determined by computerized quantification using digital images of the whole pancreatic tissue using Aperio Image Scope software. The insulin staining was calculated as the sum of staining of weak positive (N_{wp}), positive

(N_p), and strong positive (N_{sp}), and was determined as a proportion of the total area of the section (N_t) (i.e., insulin content = $[N_{wp} + N_p + N_{sp}]/N_t$).

ACE2 AND INSULIN IMMUNOFLOUORESCENCE

Paraffin-embedded mouse pancreatic tissue sections (4 μ m) were dewaxed as described previously and incubated with 10% normal goat serum (Dako) in PBS for 30 minutes. The polyclonal guinea pig anti-insulin (Dako) at 1:100 and ACE2 (Sigma-Aldrich) at 1:50 was applied, and the slides were placed in incubation chambers overnight at 4°C. Then the sections were incubated with fluorochrome-conjugated secondary antibodies; goat anti-guinea pig immunoglobulin G (IgG) H&L (Alexa Fluor 594) (Abcam) at 1:250 and goat anti-rabbit IgG H&L (Alexa Fluor 488; Abcam) at 1:250; in dark at room temperature for 1 hour. Sections were rinsed three times in PBS for 5 minutes each in dark and incubated with 1 μ g/mL 4',6-diamidino-2-phenylindole for 5 minutes, followed by mounting on a glass slide with a drop of Dako fluorescence mounting agent.

WESTERN BLOTTING FOR ACE2 PROTEIN IN LIVER

Anti-ACE2 antibody (Abcam) was used to probe liver protein extracted from mouse livers. Thereafter, PVDF membranes were incubated with polyclonal goat anti-rabbit HRP secondary antibody (Agilent Technologies). β -actin was used as loading controls. Detailed description is available in Appendix 1.

CELL CULTURE OF MOUSE β -CELLS AND α -CELLS

Insulin-producing MIN6 cells (β -cell line) and glucagon producing α -cells (α -cell line, α -TC clone 6) were grown to about 60% confluency in 24-well plates (100,000 cells per well) and were maintained in Dulbecco's modified Eagle's medium (DMEM) containing 25 mmol/L glucose, with 15% fetal bovine serum (FBS), 100 units/mL penicillin, 100 g/mL streptomycin, 100 g/mL L-glutamine, and 0.05mM beta-mercaptoethanol in humidified 5% CO₂, 95% air at 37°C. Glucagon-producing α -cells (α -cell line, α -TC1 clone 6) were similarly seeded and maintained

in DMEM containing 5.5 mmol/L glucose, with 10% FBS, 100 units/mL penicillin, 100 g/mL streptomycin, 100 g/mL L-glutamine, 15 mM HEPES, 0.1 mM nonessential amino acids, and 0.02% BSA in humidified 5% CO₂, 95% air at 37°C. The cells were infected with rAAV2/8-*ACE2* vector (1×10^9 vector genomes) or control vector (rAAV2/8-*ALB* at 1×10^9 vg) for 24 hours. Cells without the vector infection served as untreated controls. Cells were then harvested for RNA extraction and quantitative PCR for the quantification of *ACE2* messenger RNA (mRNA) expression as previously described.⁽²³⁾

STATISTICAL ANALYSIS

Means between groups were compared using one-way analysis of variance (ANOVA) with Tukey *post-hoc* test. All data are expressed as mean \pm SEM. All statistical analyses were carried out using the computer package PRISM (GraphPad Prism 7.0). $P < 0.05$ was considered statistically significant.

Results

RAAV2/8-ACE2 GENE THERAPY INCREASES ACE2 EXPRESSION IN MICE WITH NAFLD

A single dose of *ACE2* vector significantly ($P < 0.01$) increased liver *ACE2* mRNA expression by more than 50-fold (Fig. 1B), and protein content by more than 4-fold compared with those in HFHC-fed diabetic mice (Fig. 1C-F). The expression of *ACE2* in the liver of *ACE2*-treated mice was predominantly localized to hepatocytes (Fig. 1E).

ACE2 THERAPY NORMALIZES BODY MASS AND REDUCES LIVER MASS IN DIABETIC MICE

The physical appearance of animals was observed throughout the period of study, and the macroscopic features of the livers were examined at 40 weeks. Mice fed the HFHC diet without DM displayed increased body weight compared with the normal chow-fed control mice (Fig. 2A,B). In contrast, diabetic mice displayed lower body weight, compared to both normal chow-fed and HFHC-fed control mice (Fig. 2B). Livers of HFHC

diet-fed diabetic mice had a nodular appearance, suggesting advanced fibrosis. Importantly, *ACE2* treatment was associated with increased body weight and improved smoother appearance of liver without nodularity (Fig. 2A) with significantly ($P < 0.01$) reduced liver weight (Fig. 2C) compared to the diabetic mice. However, liver triglyceride content was not altered by *ACE2* therapy, and there were no differences in liver triglyceride content among the four HFHC-fed groups (Fig. 2D). In support of this, histological assessment of macrosteatosis (35 ± 5 , 35 ± 6 , 44 ± 7 , and 30 ± 6) and microsteatosis (41 ± 5 , 39 ± 6 , 27 ± 6 , and 41 ± 6) also showed no difference among the four groups of HFHC, HFHC+DM, HFHC+DM+rAAV-HSA and HFHC+DM+rAAV-*ACE2*, respectively. This suggests that the reduction in relative liver weight in *ACE2*-treated mice was not due to a reduction in liver fat content. Histological grading performed on liver H&E-stained sections, however, showed no change in inflammatory changes or hepatocyte damage (i.e., hepatocyte ballooning) among the four HFHC-fed groups (Fig. 2E).

ACE2 THERAPY IMPROVES LIVER ENZYME PROFILES IN DIABETIC NAFLD MICE

Plasma levels of alanine aminotransferase (ALT) (Fig. 3A), aspartate aminotransferase (AST) (Fig. 3B), and alkaline phosphatase (ALP) (Fig. 3C) were significantly ($P < 0.01$) elevated in HFHC-fed mice with or without diabetes when compared with chow-fed mice. Plasma ALT and AST levels were significantly ($P < 0.05$) reduced in mice treated with rAAV2/8-*ACE2* compared with diabetic mice injected with the control vector (Fig. 3A,B). There was no effect of *ACE2* on plasma ALP levels (Fig. 3C).

ACE2 THERAPY DOWN-REGULATES THE EXPRESSION OF PROINFLAMMATORY AND PROFIBROTIC CYTOKINES IN THE LIVER OF DIABETIC NAFLD MICE

Liver mRNA expression of the pro-inflammatory cytokine, interleukin-6 (*IL-6*) (Fig. 3D), was markedly ($P < 0.01$) increased in HFHC-fed diabetic control and control vector-injected diabetic mice, compared with healthy control, despite no

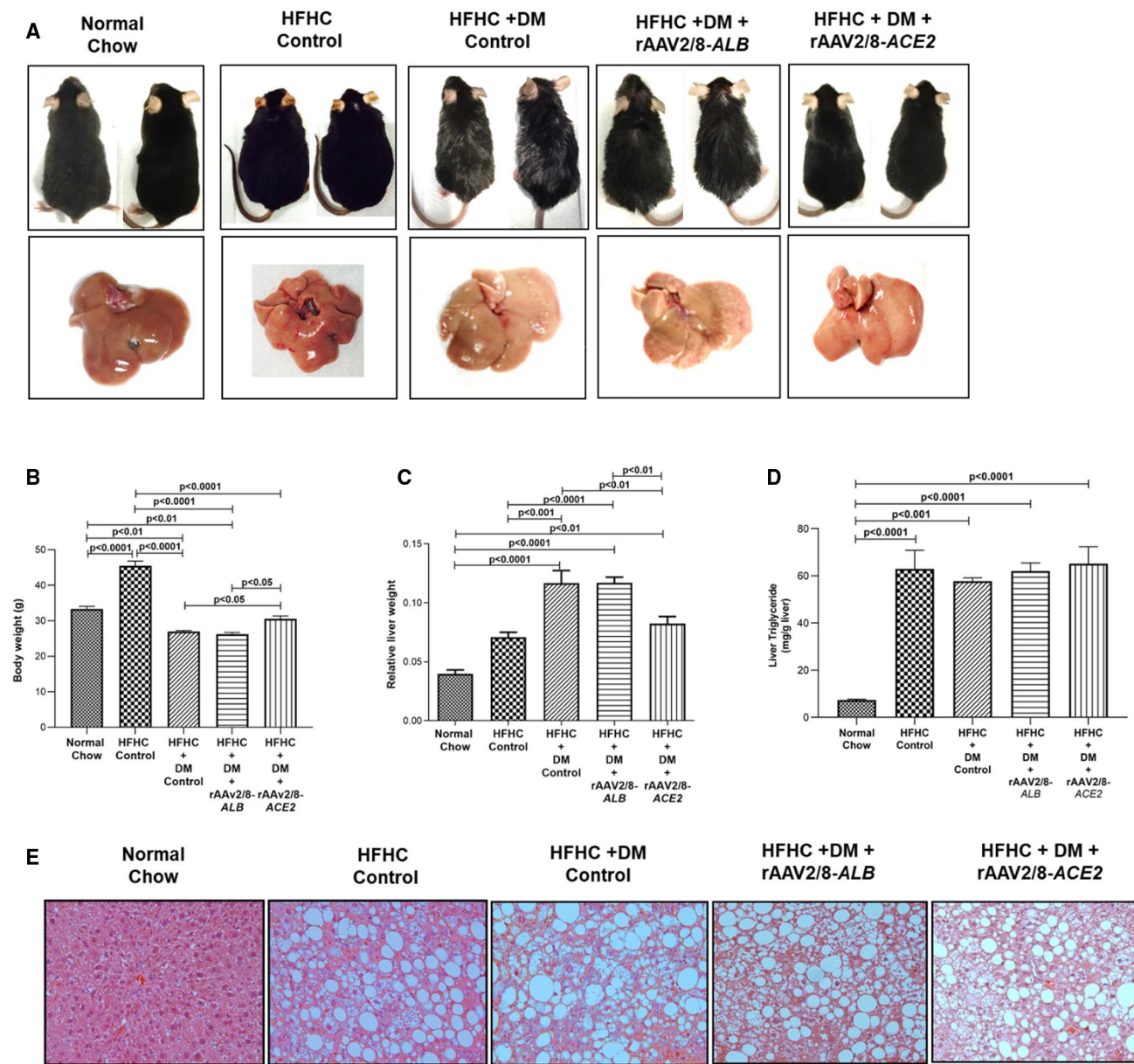


FIG. 2. Physical appearance of mice, the macroscopic appearance of the liver, body weight, the relative liver weight, and triglyceride content at 40-week advanced stage of NAFLD. (A,B) Diabetic mice had lower body weight as compared with chow-fed mice. Compared with rAAV2/8-ALB-treated diabetic mice, ACE2 treatment was associated with increased body weight, and the livers appeared smoother. (C) ACE2 treatment significantly reduced relative liver weight compared with diabetic controls. (D) Liver triglyceride content was not different between the HFHC-fed groups. (E) Representative H&E images of the livers from five groups are shown (magnification: $\times 200$). Each bar represents the mean \pm SEM profile of 5 (normal chow), 10 (HFHC groups), and 10-15 (HFHC-fed diabetic groups) mice per group as calculated by one-way ANOVA with Tukey comparison test.

histological evidence of reduced inflammation being found in ACE2-treated animals (data not shown). Similarly, mRNA expression of the profibrotic cytokines, transforming growth factor beta-1 (*TGF- β 1*) (Fig. 3E), and connective tissue growth factor (*CTGF*) (Fig. 3F) was markedly ($P < 0.01$) increased

in HFHC-fed diabetic control and control vector-injected diabetic mice, compared with healthy control. However, ACE2 therapy markedly reduced ($P < 0.05$) *IL-6*, *TGF- β 1*, and *CTGF* expressions when compared with HFHC diabetic control mice and control vector-injected diabetic mice. Notably,

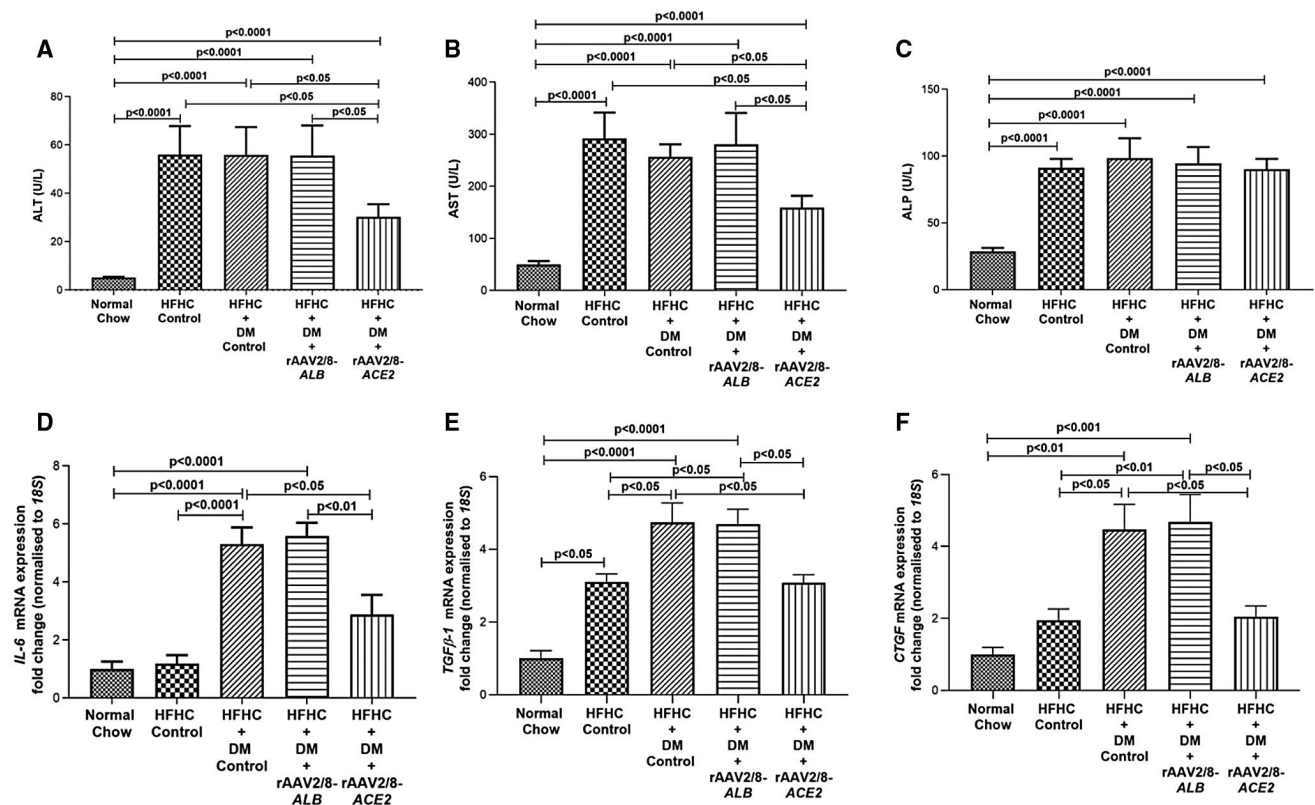


FIG. 3. Plasma concentrations of ALT, AST and ALP, and pro-inflammatory and pro-fibrotic cytokine mRNA expression in the liver. Increased plasma levels of liver enzymes ALT (A) and AST (B) in control vector-treated animals were significantly reduced by ACE2 therapy. (C) ACE2 did not affect ALP enzyme level. The mRNA expression of the pro-inflammatory cytokine, IL-6 (D), and the pro-fibrotic cytokines TGF- β 1 (E) and CTGF (F) in the liver was markedly down-regulated by ACE2 therapy compared with those of control vector-injected diabetic mice. The data are normalized to 18S. Each bar represents the mean \pm SEM profile of 5 (normal chow) or 10 (HFHC groups) and 10-15 (HFHC fed diabetic groups) mice per group as calculated by one-way ANOVA with Tukey comparison test.

in ACE2-treated animals, expression levels of these mRNA were not statistically different from the normal chow-fed mice (Fig. 3D-F).

ACE2 THERAPY REDUCES LIVER FIBROSIS IN DIABETIC NAFLD MICE

We assessed the liver expression of α -SMA, a marker of activated hepatic stellate cells (HSCs). When compared with healthy controls, α -SMA mRNA expression (Fig. 4A) and protein expression (Fig. 4B,C) were significantly ($P < 0.05$) increased in HFHC diabetic and control vector-injected diabetic mice. Importantly, a single dose of ACE2 therapy caused a more than 50% reduction in α -SMA mRNA expression (Fig. 4A) and protein expression by more than 65% (Fig. 4B,C) when compared with

the HFHC diabetic group and control vector-injected disease controls.

Collagen is a major extracellular matrix protein (ECM) in the liver. The mRNA expression of collagen 1 type 1 α 1 (*COL1A1*) was significantly ($P < 0.01$) increased in HFHC-fed mice, HFHC-fed diabetic control mice, and control vector-injected diabetic mice compared with the healthy controls (Fig. 4D). Treatment with ACE2 inhibited *COL1A1* mRNA expression by more than 50% ($P < 0.05$) in HFHC diabetic NAFLD mice in comparison with HFHC diabetic control mice and control vector-injected disease controls (Fig. 4D).

The antifibrotic effect of ACE2 in hepatic fibrosis was further confirmed by quantifying hepatic collagen protein deposition using picosirius red-stained liver sections. Collagen content was increased in HFHC-fed animals and further increased by diabetes (Fig. 4E).

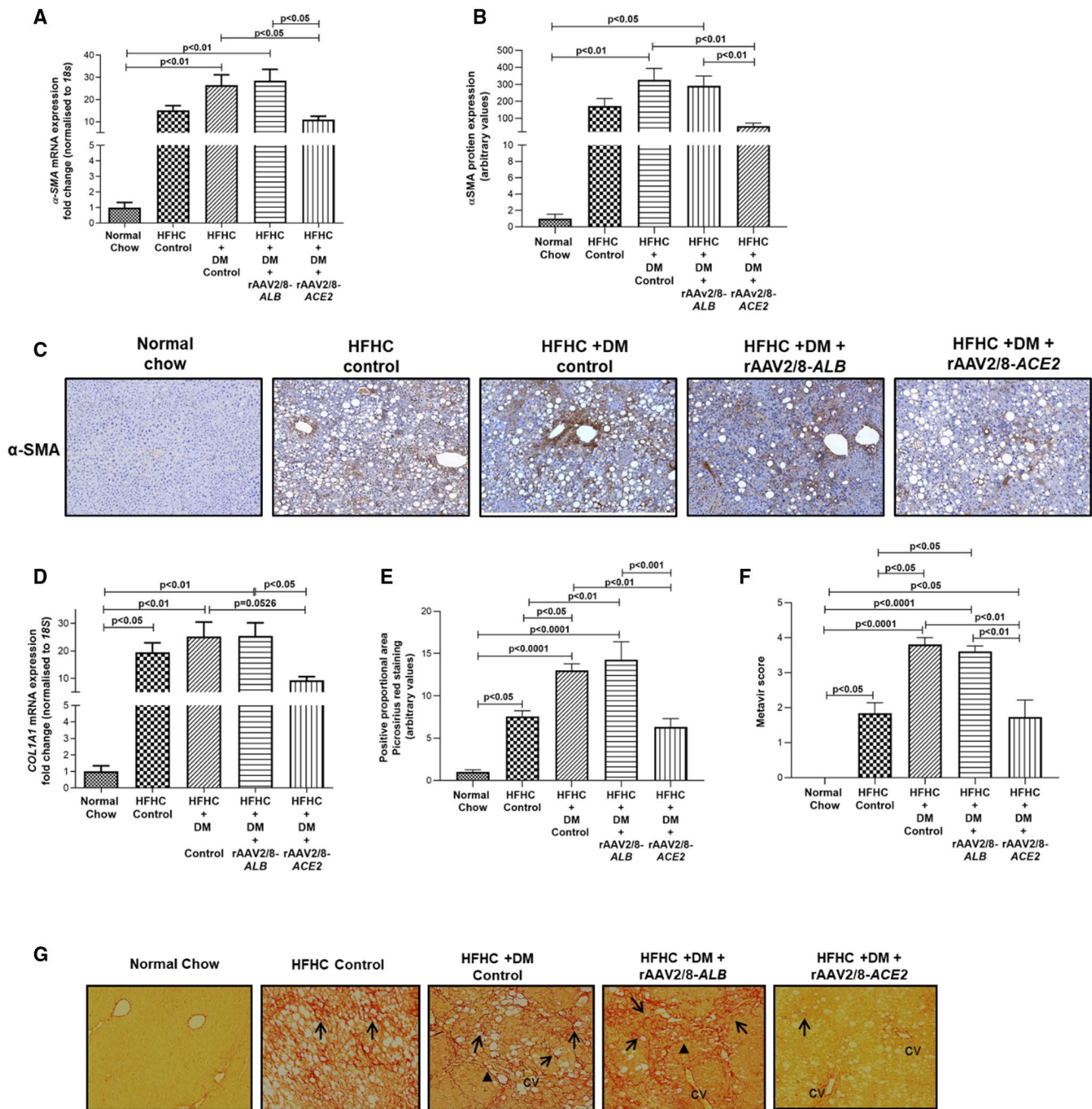


FIG. 4. ACE2 therapy reduces mRNA and protein expression of α -SMA and liver fibrosis in diabetic NAFLD mice. ACE2 gene therapy significantly reduced the expression of HSC activation marker (α -SMA) mRNA (A) and α -SMA protein content (B,C) in the livers of ACE2-treated diabetic NAFLD mice compared with HFHC diabetic and control vector-injected groups. The expression of fibrosis marker COL1A1 (D) was significantly inhibited by ACE2 therapy compared with HFHC diabetic and control vector-injected diabetic mice. Hepatic collagen content was profoundly reduced by ACE2 therapy compared with both HFHC diabetic and control vector-injected groups (E,G). Metavir fibrosis score from ACE2-treated livers was significantly lower compared with diabetic controls (F). The mRNA expression data have been normalized to 18S. Each bar represents the mean \pm SEM profile of 5 (normal chow) or 10 (HFHC groups) and 10-15 (HFHC fed diabetic groups) mice per group as calculated by one-way ANOVA with Tukey comparison test. Each bar represents the mean \pm SEM profile of 5 (normal chow) or 10 (HFHC groups) and 10-15 (HFHC fed diabetic groups) mice per group as calculated by one-way ANOVA with Tukey comparison test. Magnification: $\times 100$. Arrow, pericellular fibrosis; arrowhead, bridging fibrosis. Abbreviation: cv: central vein.

In keeping with the profound inhibition on α -SMA and COL1A1 expressions, ACE2 treatment markedly reduced collagen content by more than 50% in the liver of ACE2-treated mice compared with HFHC diabetic ($P < 0.01$) and control vector-injected (ALB) ($P < 0.001$) diabetic mice (Fig. 4E,G). Moreover, picrosirius images from HFHC diabetic and control vector-injected HFHC diabetic mice showed an extensive pericellular fibrosis (arrows) along with bridging fibrosis (arrow heads), which was markedly reduced in ACE2-treated animals (Fig. 4G).

We then assessed hepatic fibrosis using the Metavir fibrosis score on H&E and picrosirius red-stained liver sections. There was a significant increase in Metavir score with HFHC, which was further increased with diabetes in HFHC-fed mice. Consistent with the data from picrosirius-stained sections (Fig. 4E,G), Metavir scoring showed ACE2 therapy significantly ($P < 0.01$) reduced liver fibrosis in ACE2-treated animals compared with diabetic controls and control vector-injected mice (Fig. 4F).

ACE2 THERAPY INCREASES NUMBERS OF PANCREATIC β -CELL CLUSTERS, β -CELL INSULIN CONTENT AND FASTING PLASMA INSULIN, AND REDUCES GLUCOSE LEVELS IN DIABETIC NAFLD MICE

Because diabetes is a strong risk factor for advanced NAFLD and a strong predictor of cirrhosis in patients with NAFLD,^(17,18) we sought to determine the effects of STZ treatment and ACE2 therapy on pancreatic β -cells, β -cell insulin content, and plasma insulin and glucose levels. Immunohistochemical images of insulin-stained sections clearly showed brown-colored pancreatic islets, representing insulin-secreting β -cell clusters (Fig. 5A). Consistent with STZ-induced partial destruction of β -cells,⁽¹⁹⁾ the number of islets in HFHC diabetic controls and the control vector-injected diabetic group was significantly ($P < 0.05$) lower than that of the normal chow-fed control group (Fig. 5B). ACE2 therapy markedly increased ($P < 0.05$) islet numbers compared to diabetic controls with and without the control vector injection, restoring the islet numbers in ACE2-treated mice to those observed in chow-fed and HFHC controls (Fig. 5B). Notably, most islet clusters in ACE2-treated

mice appeared relatively smaller in size compared with those in HFHC control animals (Fig. 5A). Consistent with this, insulin content was significantly ($P < 0.05$) reduced in the islets of diabetic mice compared with those in normal chow-fed and HFHC control mice (Fig. 5C) and was significantly ($P < 0.05$) increased by ACE2 therapy (Fig. 5C).

Blood analysis showed that fasting plasma insulin levels were significantly reduced ($P < 0.001$) in HFHC-fed diabetic mice compared with normal chow-fed mice or HFHC-fed nondiabetic mice at both 30 weeks and 40 weeks of the respective diets (Fig. 5D). Interestingly, fasting plasma insulin levels in diabetic mice were not significantly changed from week 30 to week 40; however, mice treated with ACE2 showed increased ($P < 0.01$) fasting plasma insulin levels compared with the two groups of diabetic controls at 40 weeks and a tendency ($P = 0.12$) to increase when compared with the diabetic group at 30 weeks (Fig. 5D), suggesting that ACE2 therapy likely caused increased synthesis of insulin rather than preventing the decline of its synthesis. Fasting plasma insulin levels across groups were significantly and negatively correlated with fasting plasma glucose levels ($r = -0.78$, $P < 0.001$), which rose from a normal range in normal chow or HFHC-fed mice to significantly higher ($P < 0.01$) levels in diabetic mice (Fig. 5E). However, diabetic mice treated with ACE2 had significantly ($P < 0.05$) reduced (>30%) fasting glucose levels compared to diabetic mice with or without the control vector injection at 40 weeks of HFHC diet. Additionally, fasting plasma glucose levels in ACE2-treated mice were not different from those in the diabetic group at 30 weeks of HFHC diet, suggesting that ACE2 therapy prevented the rise of plasma glucose during the course of disease progression (Fig. 5E).

ACE2 AND INSULIN EXPRESSION IN THE PANCREATIC TISSUE

We have previously reported that the liver-targeted ACE2 vector used in these experiments did not increase ACE2 expression in other major organs such as heart, kidneys, lungs, brain, or small intestine.⁽¹³⁾ However, because ACE2 therapy had a positive impact on glycemic control by increasing β -cell insulin content and thereby increasing plasma insulin levels, we explored the promoter (ApoE/hAAT)

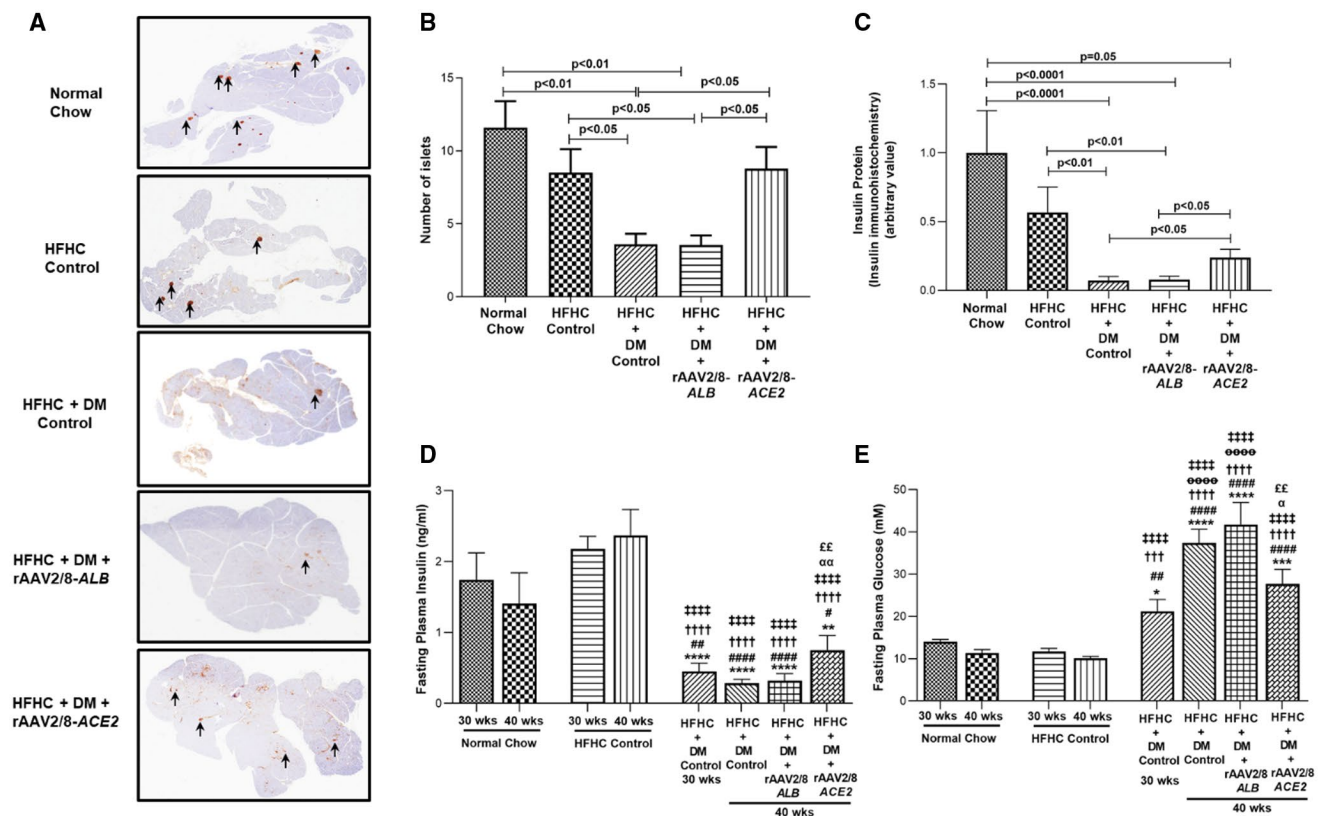


FIG. 5. ACE2 therapy is associated with increased pancreatic islet mass and insulin content, higher plasma insulin, and lower glucose levels in diabetic mice with NAFLD. (A) Insulin-secreting pancreatic β -cell islets in normal chow, HFHC control mice, diabetic control, and diabetic mice injected with control ALB vector or ACE2 vector are shown. (B) The number of islets was significantly increased in mice with ACE2 therapy compared with control vector-injected mice. (C) Insulin content in β -cells was significantly higher in ACE2-treated mice compared with control vector-injected diabetic mice. (D) Fasting plasma insulin levels were higher (>60%) in ACE2-treated diabetic NAFLD mice than control vector-injected diabetic NAFLD mice. (E) Increased plasma insulin levels in ACE2-treated mice were accompanied by reduced (>30%) fasting plasma glucose levels compared with control vector-injected mice. Each bar represents the mean \pm SEM profile of 5 (normal chow), 10 (HFHC nondiabetic), and 10-15 (HFHC diabetic groups) mice per group as calculated by one-way ANOVA with Tukey's multiple comparison test. Magnification: $\times 100$. * $P < 0.05$, ** $P < 0.01$, *** $P < 0.001$, and **** $P < 0.0001$ versus normal chow-30 weeks; # $P < 0.05$, ## $P < 0.01$, and ### $P < 0.0001$ versus normal chow-40 weeks; ††† $P < 0.001$ and †††† $P < 0.0001$ versus HFHC control-30 weeks; ‡‡‡‡ $P < 0.0001$ versus HFHC control-40 weeks; ††††† $P < 0.0001$ versus HFHC+DM control-30 weeks; ° $P < 0.05$ and °° $P < 0.01$ versus HFHC+DM control-40 weeks; and ††† $P < 0.01$ versus HFHC+DM+rAAV2/8-ALB-40 weeks.

activity in pancreatic islet cells. Immunohistochemical quantification showed that ACE2 protein expression in the islets was significantly ($P < 0.01$) higher in ACE2-treated NAFLD mice compared with the two groups of diabetic control mice and was similar to the level in nondiabetic animals (Fig. 6A,C). Thus, ACE2 gene therapy normalized ACE2 expression in diabetic NAFLD mice whose pancreatic islets were damaged by STZ injections. To further confirm the vector specificity for β -cells, we transduced MIN6 β cells with the ACE2 vector. Angiotensin-converting enzyme 2 mRNA expression was significantly up-regulated in ACE2-treated MIN6 cells compared

with untreated ($P < 0.001$) and control ALB vector-treated ($P < 0.01$) cells (Fig. 6B). To explore whether the vector transduces other cell types in the islets, we also used glucagon-secreting α -cells, α -TC clone 6. Similar to β -cells, we found that α -TC clone 6 cells transduced with the ACE2 vector had significantly up-regulated ACE2 mRNA expression compared with untreated ($P < 0.001$) and control ALB vector-treated ($P < 0.001$) cells (Fig. 6B), suggesting that the vector transduces α -cells in the islets.

We then assessed co-localization of islet insulin and ACE2 protein in the pancreas of mice. There was a similar expression pattern of insulin to that

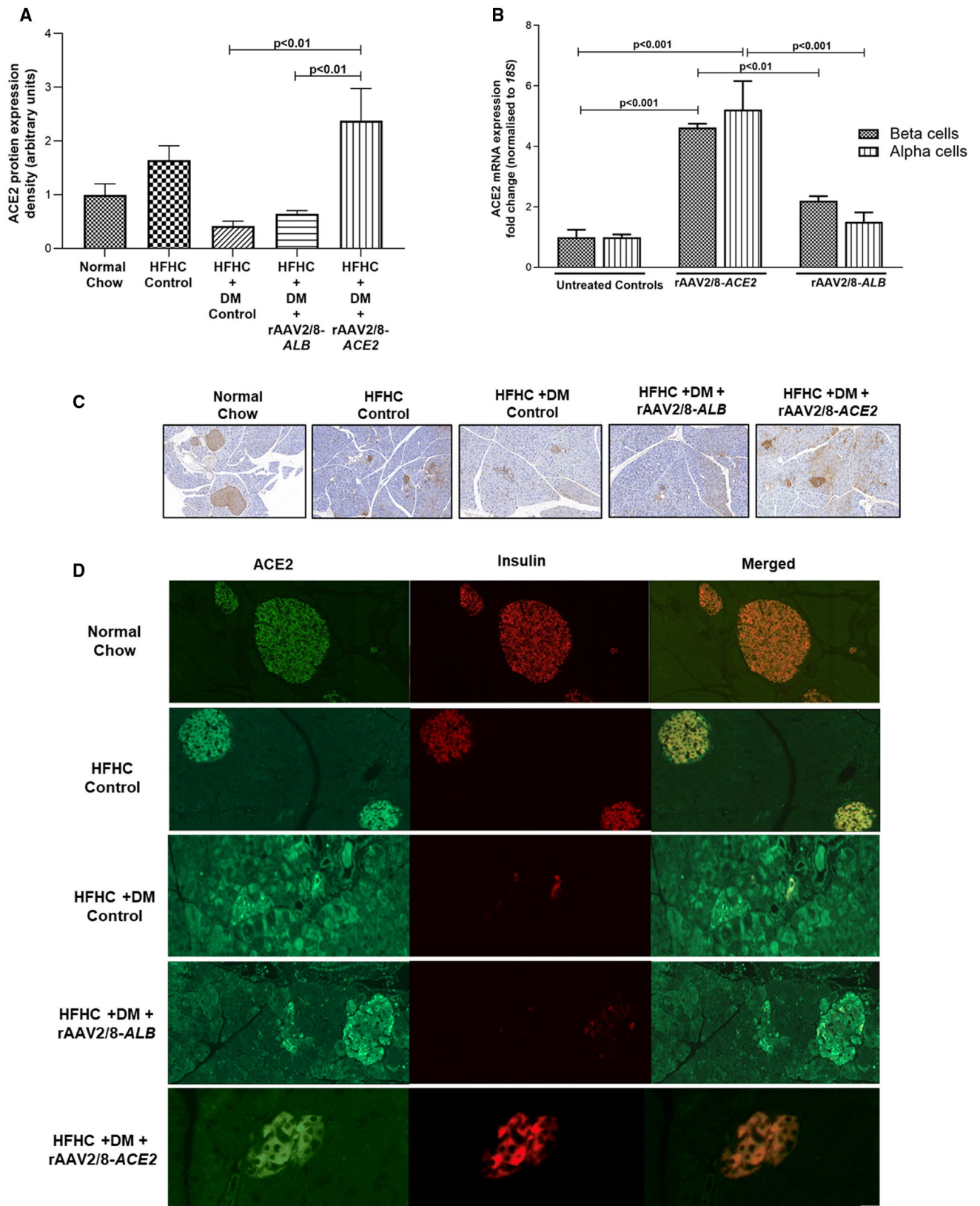


FIG. 6. ACE2 protein expression and co-localization with insulin in pancreatic islet cells. (A,C) ACE2 protein expression was lower in diabetic NAFLD mice compared with those of healthy and nondiabetic NAFLD mice. Importantly, ACE2 therapy markedly increased ACE2 expression in the islets of diabetic NAFLD mice. (B) Infection of both β -cells and α -cells with the ACE2 vector increased ACE2 expression in both cell types. (D) ACE2 was co-localized with insulin in the β -cells, and increased ACE2 expression with ACE2 therapy was associated with increased insulin expression in diabetic NAFLD mice. Each bar represents the mean \pm SEM profile of 5 (normal chow), 10 (HFHC nondiabetic), and 10-15 (HFHC diabetic) mice per group as calculated by one-way ANOVA with Tukey's multiple comparison test. ACE2 immunohistochemistry, magnification $\times 100$; immunofluorescence sections, 20 μm ; $n = 3$ independent experiments per cell type.

of ACE2, with higher expression in the islet cells of both normal chow-fed and HFHC-fed nondiabetic NAFLD mice compared with expression levels in diabetic mice whose β -cell population was partially destroyed by STZ injections (Fig. 6D). Strikingly, there was a strong ACE2 expression in the islets of ACE2-treated diabetic mice, and it appears that its expression was primarily colocalized with that of insulin in the β -cells (Fig. 6D). This increased expression of ACE2 and insulin in islet β -cells of ACE2-treated diabetic mice provided further evidence that ACE2 has a direct stimulatory effect on the synthesis and secretion of insulin in diabetic mice with subsequent improvement in hyperglycemia.

Discussion

The major aim of this study was to elucidate the therapeutic effects of AAV-mediated liver-targeted ACE2 gene therapy on liver injury and fibrosis in advanced NAFLD/NASH. In agreement with our published studies,^(10,13) ACE2 therapy resulted in more than four-fold increase in ACE2 protein expression, improved liver biochemistry, and prevented the development of advanced liver disease in a long-term model of diabetic NAFLD.

Numerous rodent models of NAFLD have been described in the literature, which include models developed using nutritional, genetic, toxic, and viral factor modification.^(25,26) We used a nutritional model of NAFLD induced by feeding mice with a HFHC diet for 40 weeks. This model demonstrates slow disease progression, and many of the comorbidities observed in human NAFLD are present in this model, including obesity, dyslipidemia, insulin resistance, and impaired glycemic control.⁽²⁷⁾ However, the HFHC diet alone is not sufficient to induce severe NASH and advanced liver fibrosis in animal models,⁽¹⁹⁾ and because diabetes is a strong risk factor

that exacerbates NAFLD and is a predictor of cirrhosis in patients with NAFLD,^(18,28) we superimposed chemical-induced diabetes in our model⁽¹⁹⁾ to drive NASH and worsen liver fibrosis (Figs. 3 and 4).

ACE2 gene therapy induced striking effects on the whole-body phenotype of the animals and the macroscopic appearance of the livers. As expected, diabetic mice lost considerable weight, with an apparent reduction in adipose tissue mass, and a nodular appearance was observed in the livers of several diabetic NAFLD mice, suggesting that they developed early cirrhosis (Fig. 2). In marked contrast, ACE2 therapy changed the physical appearance of the diabetic NAFLD mice with body weight similar to normal chow-fed mice and relative liver weight similar to nondiabetic NAFLD mice. This may suggest that the ACE2-induced improvement in glycemic control likely resulted in the restoration and maintenance of adipose tissue mass.

Perpetuation of inflammation in chronic liver disease is driven by continuous exposure of the liver parenchyma to increased levels of proinflammatory cytokines secreted by inflammatory cells.^(10,13,22,29) Proinflammatory cytokine *IL-6* is closely associated with liver injury.⁽³⁰⁾ We showed that in comparison with healthy mice, *IL-6* levels—which were markedly up-regulated in diabetic NAFLD mice—were significantly reduced by ACE2 therapy, although no such changes were observed histologically. It is known that proinflammatory cytokines lead to activation of profibrogenic stimuli such as *CTGF*, and in particular, *TGF- β 1*, a potent profibrogenic cytokine secreted by both Kupffer cells and HSCs.^(13,29) Release of profibrogenic cytokines has an autocrine and paracrine action by activating quiescent HSCs into a myofibroblastic phenotype that secretes excess ECM.⁽²⁹⁾ Consistent with our previous findings,^(10,13,22) ACE2 therapy reduced expression of *CTGF* and *TGF- β 1*, leading to the inhibition of HSC activation, as reflected by a more than 60% reduction in α -SMA

gene and protein expression. In keeping with the reduced expression of α -SMA, we found that in the livers of ACE2-treated mice, the expression of collagen, a major ECM protein secreted by activated HSCs, was greatly reduced, and these changes were associated with a more than 60% reduction in fibrosis in these mice compared with control vector-injected animals (Fig. 4). Mechanistically, ACE2 breaks down hepatic profibrotic peptide angiotensin II to antifibrotic angiotensin-(1-7) peptide, and this is associated with reduced generation of reactive oxygen species through activation of the nicotinamide adenine dinucleotide phosphate (reduced form) oxidase pathway which is a key mechanism through which angiotensin II activates stellate cells and drives liver inflammation and fibrosis.⁽¹³⁾

It was of major interest to evaluate the effects of this ACE2 therapy on glycemic control in diabetic NAFLD mice, because diabetes promotes NAFLD progression to NASH and cirrhosis.^(28,31) In this study, a single injection of an AAV vector carrying the ACE2 gene was associated with an increase in pancreatic islet numbers and increased pancreatic β -cell insulin content, which resulted in higher plasma insulin levels compared with control vector-injected diabetic NAFLD mice. This was accompanied by a more than 30% reduction in plasma glucose levels in ACE2-treated animals (Fig. 5). Moreover, a 30% reduction in plasma glucose level as a response to ACE2 therapy is clinically significant, because lowering plasma glucose level is expected to reduce the progression of NAFLD to NASH and cirrhosis.⁽²⁸⁾ However, ACE2-treated animals still remained significantly hyperglycemic; thus, the marked improvement in liver fibrosis in response to ACE2 therapy was unlikely to be due to amelioration of diabetes alone.

The AAV vector we constructed to overexpress ACE2 was pseudo-serotyped with the highly murine liver-trophic serotype 8 capsid, which we had previously reported as liver-specific, because ACE2 transcription was driven by the liver-specific ApoE/hAAT enhancer-promoter without targeting other major organs such as heart, kidneys, lungs, brain, or small intestine.⁽¹³⁾ However, in the present study, ACE2 protein was significantly higher in the islets of ACE2-treated diabetic mice compared with those of the other diabetic groups (Figs. 5 and 6), suggesting that the AAV serotype 8 vector recognizes and transduces islet cells, leading to ACE2 transcription driven by

ApoE/hAAT enhancer-promoter. This was supported by independent studies in cultured α -cells and β -cells that showed increased expression of ACE2 following rAAV2/8-ACE2 vector administration. This is not surprising, because the pancreas and liver have the same embryonic origin^(32,33); thus, both may harbor the AAV serotype 8 receptor and the transcription machinery involving the same promoter elements. Supporting pancreatic tropism of AAV serotype 8 vector, a previous study showed that intraperitoneal administration of this vector-carrying green fluorescent protein gene into mice produced insulin promoter-driven high expression of the protein in the islet cells.⁽³⁴⁾

One mechanism by which ACE2 therapy improved glycemic control appeared to be by increasing islet cell numbers. This appears likely due to a local effect of ACE2 in stimulating the regrowth of the islet cell population, as a major source of new β -cells in adult mice is pre-existing β -cells rather than pluripotent stem cells.⁽³⁵⁾ It is therefore unlikely that ACE2 therapy had an inhibitory effect on STZ-induced β -cell loss, because the drug was administered 15 weeks before ACE2 therapy.^(19,36) ACE2 therapy may also have directly improved β -cell function and insulin secretion as a result of its effects on angiotensin peptide levels. Ang II inhibits insulin synthesis and secretion by β -cells^(37,38); thus, ACE2, which degrades Ang II, is likely to have reduced local Ang II levels,⁽¹³⁾ leading to increased insulin production.⁽³⁷⁾ Furthermore, the product of Ang II degradation by ACE2 is Ang-(1-7), a peptide that has both anti-inflammatory and antioxidant properties^(10,13) and is a potent stimulant of β -cell function, insulin synthesis, and secretion.^(39,40) Although an increased ratio of Ang-(1-7) to Ang II in the islet microenvironment of ACE2-treated animals helps improve insulin synthesis and/or secretion, Ang-(1-7)—which may also be possibly released into the islet microcirculation—can reach other organs such as adipose and muscle tissues where Ang-(1-7) may improve insulin resistance by modulating insulin actions and reducing inflammation.⁽⁴¹⁾ Because present studies were primarily designed to investigate the therapeutic efficacy of ACE2 in diabetic NAFLD, further studies are warranted to investigate whether organ-specific ACE2 overexpression improves peripheral insulin resistance through increased circulating Ang-(1-7) peptide levels in diabetes. These findings thus provide strong evidence that a single administration of ACE2 vector produces long-term therapeutic

effects on glycemic control, which may have partly contributed to the beneficial effect of ACE2 on NAFLD progression to liver fibrosis in diabetic NAFLD animals. It should be noted, however, that while the chemical-induced diabetic model we used drove NASH and worsened liver fibrosis, this model with a reduced population of pancreatic β -cells is more akin to type 1 diabetes than the type 2 diabetes generally associated with NAFLD. However, it did produce histological changes typical of those seen in patients with diabetes with advanced NAFLD.

In support of our findings, when injected directly into the pancreas, adenovirus-carrying human ACE2 improved glycemic control and increased islet insulin content and β -cell proliferation with a reduction in β -cell apoptosis in diabetic db/db mice.⁽⁴²⁾ However, the antidiabetic effect of ACE2 delivered by adenoviral vector in this manner was not sustained, and the invasive nature of the treatment using five intrapancreatic injections of adenovirus limits the clinical applicability of this approach.⁽⁴²⁾

Gene therapy technology is rapidly evolving, and there is an imminent possibility in the future of gene-therapy approaches to cure not only genetic disorders but also nongenetic disorders.^(43,44) However, gene-therapy clinical studies of genetic disorders are often met with a challenge of achieving a long-term therapeutic effect due to immune responses directed against the vector and/or the transcribed protein product.⁽⁴⁴⁾ Nonetheless, treatment of patients with hemophilia B with liver-directed AAV8 vector-carrying human blood clotting factor IX (FIX) was successful and enabled most patients to reduce the use of FIX concentrate by more than 86%.⁽⁴⁵⁾ Ongoing development of AAV capsid technology is to deliver AAV vector configurations with increasing human liver tropism, which will extend therapeutic reach to a greater number of liver-disease phenotypes while simultaneously reducing the vector doses required.^(46,47) This includes nongenetic disorders such as NAFLD/NASH, in which relatively high proportions of the hepatic cell mass will need to be transduced for optimal therapeutic effect and bodes well for clinical translation in the near term.⁽⁴⁴⁾

In summary, rAAV2/8-ACE2 gene therapy markedly improves liver injury and fibrosis in diabetic mice with NAFLD/NASH. We demonstrated that this therapy acts in the diabetic pancreas to increase islet numbers and insulin content, and this is associated with improved glycemic control. Although ACE2-treated

animals still had significant hyperglycemia, this improvement in blood glucose levels likely contributed to the beneficial effect of ACE2 on NAFLD progression to liver fibrosis. We therefore conclude that the protective axis of the RAS has potential as a therapeutic target in diabetic NAFLD, as up-regulation of ACE2 activity by ACE2 gene therapy inhibits both liver fibrosis and improves glycemic control.

Acknowledgment: The authors would like to acknowledge the staff of the University of Melbourne histology platform and APN histopathology service for their technical assistance on immunohistochemistry, and Christine Yee for the assistance with cell culture experiments.

Appendix 1

BIOCHEMICAL ASSESSMENT OF LIVER FUNCTION AND HEPATIC TRIGLYCERIDE CONTENT

Plasma alanine transaminase (ALT), aspartate transaminase (AST), and alkaline phosphatase (ALP) were measured using Beckman Coulter LX20 Autoanalyser (Pasadena, CA) at Austin Pathology, Austin Health.

Hepatic lipids were extracted in chloroform:methanol (2:1 vol/vol), and the phases were separated with 4 mmol/L $MgCl_2$. Triglyceride content was determined by colorimetric assay (Triglycerides GPAP; Roche Diagnostics).⁽⁴⁸⁾

ACE2 AND α -SMA IMMUNOHISTOCHEMISTRY

ACE2

Staining was also performed on 4- μ m sections of paraffin-embedded mouse liver/pancreas tissue mounted on silane-coated glass slides. Specimens were dewaxed twice in 100% histolene for 5 minutes each and dehydrated in graded ethanol (three times in 100% and then once in 95% for 3 minutes each). The sections were washed thoroughly in running tap water for 20 minutes followed by washing in Milli-Q water and 1 \times PBS for 5 minutes each on a rocker. Heat-induced antigen retrieval was performed by immersing the slides in citrate buffer for 15 minutes in a microwave. Endogenous peroxidase activity in the liver specimens

was removed by application of peroxidase block solution at RT for 5 minutes. Washing steps with Milli-Q water and 1 × PBS were repeated as explained previously. The primary antibody to ACE2 (Abcam) at a concentration of 1:1,500 Tris-HCl containing 1% BSA (Trace Biosciences, New Zealand) was applied, and the slides were incubated overnight at 4°C.

α-SMA

The biotinylated primary antibody to α-SMA (monoclonal 1A4) (Dako) at a concentration of 1 in 50 in Tris-HCl containing 1% BSA (Trace Biosciences) was applied, and the slides were left at RT for 15 minutes. Once the incubation with each primary antibody was completed, the sections were washed using Milli-Q water and 1 × PBS and incubated with streptavidin peroxidase at RT for 15 minutes. Sections were again washed with Milli-Q water and 1 × PBS, and peroxidase conjugates were subsequently localized using DAB + substrate chromogen (Sigma-Aldrich) at RT for 15 minutes. The sections were rinsed with Milli-Q water and stained with hematoxylin (Sigma-Aldrich) for 1 minute at RT as described previously. The relative staining in each group was determined by computerized quantification (Fiji Image J) in a total of 10 fields per liver/pancreas sample at ×200 magnification and averaged in a blinded fashion.

Western Blotting

Liver tissue samples were homogenized in 0.5 mL of ice-cold lysis buffer and 1 × PhosSTOP phosphatase inhibitor cocktail tablet solution (Hoffmann-La Roche) and then centrifuged at 72,000 × g using Optima TLX ultracentrifuge (Beckman Coulter) for 1 hour at 4°C. After centrifugation, the resultant supernatant was kept as cytosolic samples, whereas the pellet was resuspended and sonicated in 0.5 mL of ice-cold lysis buffer and kept as membrane samples. Then, membrane samples (~50 µg) were subject to western blotting. Anti-ACE2 antibody (Abcam) was used to probe liver protein extracted from mouse livers. Thereafter, polyvinylidene fluoride membranes were incubated with polyclonal goat anti-rabbit horseradish peroxidase secondary antibody (Agilent Technologies). β-actin was used as loading controls.

Blots probed with protein were developed in enhanced chemiluminescence reagent (Thermo Fisher

Scientific, Waltham, MA). Intensities of the digitally detected bands were evaluated densitometrically using Gel Doc XR System (Bio-Rad, Hercules, CA).

REFERENCES

- 1) World Health Organization. Global Health Estimates 2014 Summary Tables: Deaths by Cause, Age and Sex. Geneva, Switzerland: WHO; 2014.
- 2) Leung C, Rivera L, Furness JB, Angus PW. The role of the gut microbiota in NAFLD. *Nat Rev Gastroenterol Hepatol* 2016;13:412-425.
- 3) Wong RJ, Cheung R, Ahmed A. Nonalcoholic steatohepatitis is the most rapidly growing indication for liver transplantation in patients with hepatocellular carcinoma in the U.S. *Hepatology* 2014;59:2188-2195.
- 4) Kleiner DE, Brunt EM, Van Natta M, Behling C, Contos MJ, Cummings OW, et al. Design and validation of a histological scoring system for nonalcoholic fatty liver disease. *Hepatology* 2005;41:1313-1321.
- 5) Fernando DH, Forbes JM, Angus PW, Herath CB. Development and progression of non-alcoholic fatty liver disease: the role of advanced glycation end products. *Int J Mol Sci* 2019;20:5037.
- 6) London RM, George J. Pathogenesis of NASH: animal models. *Clin Liver Dis* 2007;11:55-74.
- 7) Ratziu V, Caldwell S, Neuschwander-Tetri BA. Therapeutic trials in nonalcoholic steatohepatitis: insulin sensitizers and related methodological issues. *Hepatology* 2010;52:2206-2215.
- 8) Younossi ZM, Stepanova M, Ong J, Trimble G, AlQahtani S, Younossi I, et al. Nonalcoholic steatohepatitis is the most rapidly increasing indication for liver transplantation in the United States. *Clin Gastroenterol Hepatol* 2021;19:580-589.e585.
- 9) Paizis G, Cooper ME, Schembri JM, Tikellis C, Burrell LM, Angus PW. Up-regulation of components of the renin-angiotensin system in the bile duct-ligated rat liver. *Gastroenterology* 2002;123:1667-1676.
- 10) Rajapaksha IG, Gunarathne LS, Asadi K, Cunningham SC, Sharland A, Alexander IE, et al. Liver-targeted angiotensin converting enzyme 2 therapy inhibits chronic biliary fibrosis in multiple drug-resistant gene 2-knockout mice. *Hepatology* 2019;3:1656-1673.
- 11) Klein S, Herath CB, Schierwagen R, Grace J, Haltenhof T, Uschner FE, et al. Hemodynamic effects of the non-peptidic angiotensin-(1-7) agonist AVE0991 in liver cirrhosis. *PLoS One* 2015;10:e0138732.
- 12) Tipnis SR, Hooper NM, Hyde R, Karran E, Christie G, Turner AJ. A human homolog of angiotensin-converting enzyme. Cloning and functional expression as a captopril-insensitive carboxypeptidase. *J Biol Chem* 2000;275:33238-33243.
- 13) Mak KY, Chin R, Cunningham SC, Habib MR, Torresi J, Sharland AF, et al. ACE2 therapy using adeno-associated viral vector inhibits liver fibrosis in mice. *Mol Ther* 2015;23:1434-1443.
- 14) Rajapaksha IG, Gunarathne LS, Angus PW, Herath CB. Update on new aspects of the renin-angiotensin system in hepatic fibrosis and PHT: implications for novel therapeutic options. *J Clin Med* 2021;10:702.
- 15) Lubel J, Herath C, Tchongue J, Grace J, Jia Z, Spencer K, et al. Angiotensin-(1-7), an alternative metabolite of the renin-angiotensin system, is up-regulated in human liver disease and has antifibrotic activity in the bile-duct-ligated rat. *Clin Sci* 2009;117:375-386.
- 16) Warner FJ, Rajapaksha H, Shackel N, Herath CB. ACE2: from protection of liver disease to propagation of COVID-19. *Clin Sci (Lond)* 2020;134:3137-3158.

- 17) Calzadilla Bertot L, Adams LA. The natural course of non-alcoholic fatty liver disease. *Int J Mol Sci* 2016;17:774.
- 18) Strey CBM, Carli LAD, Pioner SR, Fantinelli M, Gobatto SS, Bassols GF, et al. Impact of diabetes mellitus and insulin on non-alcoholic fatty liver disease in the morbidly obese. *Ann Hepatol* 2018;17:585-591.
- 19) Lo L, McLennan SV, Williams PF, Bonner J, Chowdhury S, McCaughan GW, et al. Diabetes is a progression factor for hepatic fibrosis in a high fat fed mouse obesity model of non-alcoholic steatohepatitis. *J Hepatol* 2011;55:435-444.
- 20) Mohamed J, Nazratun Nafizah AH, Zariyantey AH, Budin SB. Mechanisms of diabetes-induced liver damage: the role of oxidative stress and inflammation. *Sultan Qaboos University Medical J* 2016;16:e132-e141.
- 21) Nakagawa H. Recent advances in mouse models of obesity- and nonalcoholic steatohepatitis-associated hepatocarcinogenesis. *World J Hepatol* 2015;7:2110-2118.
- 22) Rajapaksha IG, Angus P, Herath C. Current therapies and novel approaches for biliary diseases. *World J Gastrointestinal Pathophysiol* 2019;10:1-10.
- 23) Rajapaksha IG, Mak KY, Huang P, Burrell LM, Angus PW, Herath CB. The small molecule drug diminazene aceturate inhibits liver injury and biliary fibrosis in mice. *Sci Rep* 2018;8:10175.
- 24) de la M, Hall P, Kirsch R. Pathology of hepatic steatosis, NASH and related conditions. In: *Fatty Liver Disease*. Hoboken, NJ: Blackwell Publishing Ltd; 2007:13-22.
- 25) Koteish A, Mae DA. Animal models of steatohepatitis. *Best Pract Res Clin Gastroenterol* 2002;16:679-690.
- 26) Farrell GC, Teoh NC, McCuskey RS. Hepatic microcirculation in fatty liver disease. *Anat Rec* 2008;291:684-692.
- 27) Kanuri G, Bergheim I. In vitro and in vivo models of non-alcoholic fatty liver disease (NAFLD). *Int J Mol Sci* 2013;14:11963-11980.
- 28) Calzadilla Bertot L, Adams LA. The natural course of NAFLD. *Int J Mol Sci* 2016;17.
- 29) Bataller R, Brenner DA. Liver fibrosis. *J Clin Invest* 2005;115:209-218.
- 30) Yamaguchi K, Itoh Y, Yokomizo C, Nishimura T, Niimi T, Fujii H, et al. Blockade of interleukin-6 signaling enhances hepatic steatosis but improves liver injury in methionine choline-deficient diet-fed mice. *Lab Invest* 2010;90:1169-1178.
- 31) Tomah S, Alkhoury N, Hamdy O. Nonalcoholic fatty liver disease and type 2 diabetes: where do Diabetologists stand? *Clin Diabetes Endocrinol* 2020;6:9.
- 32) Wandzioch E, Zaret KS. Dynamic signaling network for the specification of embryonic pancreas and liver progenitors. *Science* 2009;324:1707-1710.
- 33) Jennings RE, Berry AA, Strutt JP, Gerrard DT, Hanley NA. Human pancreas development. *Development* 2015;142:3126-3137.
- 34) Wang Z, Zhu T, Rehman KK, Bertera S, Zhang J, Chen C, et al. Widespread and stable pancreatic gene transfer by adeno-associated virus vectors via different routes. *Diabetes* 2006;55:875-884.
- 35) Dor Y, Brown J, Martinez OI, Melton DA. Adult pancreatic beta-cells are formed by self-duplication rather than stem-cell differentiation. *Nature* 2004;429:41-46.
- 36) Charlton MR, Burns JM, Pedersen RA, Watt KD, Heimbach JK, Dierkhising RA. Frequency and outcomes of liver transplantation for nonalcoholic steatohepatitis in the United States. *Gastroenterology* 2011;141:1249-1253.
- 37) Chu KY, Leung PS. Angiotensin II type 1 receptor antagonism mediates uncoupling protein 2-driven oxidative stress and ameliorates pancreatic islet beta-cell function in young type 2 diabetic mice. *Antioxid Redox Signal* 2007;9:869-878.
- 38) Leung PS. The physiology of a local renin-angiotensin system in the pancreas. *J Physiol* 2007;580:31-37.
- 39) He J, Yang Z, Yang H, Wang LJ, Wu H, Fan Y, et al. Regulation of insulin sensitivity, insulin production, and pancreatic β cell survival by angiotensin-(1-7) in a rat model of streptozotocin-induced diabetes mellitus. *Peptides* 2015;64:49-54.
- 40) Sahr A, Wolke C, Maczewsky J, Krippeit-Drews P, Tetzner A, Drews G, et al. The angiotensin-(1-7)/Mas axis improves pancreatic β -cell function in vitro and in vivo. *Endocrinology* 2016;157:4677-4690.
- 41) Lelis DF, Freitas DF, Machado AS, Crespo TS, Santos SHS. Angiotensin-(1-7), adipokines and inflammation. *Metabolism* 2019;95:36-45.
- 42) Bindom SM, Hans CP, Xia H, Boulares AH, Lazartigues E. Angiotensin I-converting enzyme type 2 (ACE2) gene therapy improves glycemic control in diabetic mice. *Diabetes* 2010;59:2540-2548.
- 43) Mak KY, Rajapaksha IG, Angus PW, Herath CB. The adeno-associated virus—a safe and promising vehicle for liver-specific gene therapy of inherited and non-inherited disorders. *Curr Gene Ther* 2017;17:4-16.
- 44) Ginn SL, Amaya AK, Alexander IE, Edelstein M, Abedi MR. Gene therapy clinical trials worldwide to 2017: an update. *J Gene Med* 2018;20:e3015.
- 45) Nathwani AC, Reiss UM, Tuddenham EGD, Rosales C, Chowdhury P, McIntosh J, et al. Long-term safety and efficacy of factor IX gene therapy in hemophilia B. *N Engl J Med* 2014;371:1994-2004.
- 46) Lisowski L, Dane AP, Chu K, Zhang Y, Cunningham SC, Wilson EM, et al. Selection and evaluation of clinically relevant AAV variants in a xenograft liver model. *Nature* 2014;506:382-86.
- 47) Paulk NK, Pekrun K, Zhu E, Nygaard S, Li B, Xu J, et al. Bioengineered AAV capsids with combined high human liver transduction in vivo and unique humoral seroreactivity. *Mol Ther* 2018;26:289-303.
- 48) Montgomery MK, Bayliss J, Devereux C, Bezawork-Geleta A, Roberts D, Huang C, et al. SMOC1 is a glucose-responsive hepatokine and therapeutic target for glycemic control. *Sci Transl Med* 2020;12:eaaz8048.

Author names in bold designate shared co-first authorship.